

This article was downloaded by:

On: 26 January 2011

Access details: *Access Details: Free Access*

Publisher *Taylor & Francis*

Informa Ltd Registered in England and Wales Registered Number: 1072954 Registered office: Mortimer House, 37-41 Mortimer Street, London W1T 3JH, UK



Liquid Crystals

Publication details, including instructions for authors and subscription information:

<http://www.informaworld.com/smpp/title~content=t713926090>

Stationary noise of the light scattered by a polymer-dispersed liquid crystal

P. Allia^{ab}; C. Oldano^{ab}; M. Rajteri^{ab}; P. Taverna^{ab}; L. Trossi^{ab}; R. Aloe^{cd}

^a Dipartimento di Fisica, Politecnico di Torino, Torino, Italy ^b Consorzio INFM, Research Unit of Torino Politecnico, Torino, Italy ^c Dipartimento di Chimica, Università della Calabria, Rende, Italy ^d Consorzio INFM, Research Unit of Cosenza, Rende, Italy

To cite this Article Allia, P. , Oldano, C. , Rajteri, M. , Taverna, P. , Trossi, L. and Aloe, R.(1995) 'Stationary noise of the light scattered by a polymer-dispersed liquid crystal', *Liquid Crystals*, 18: 4, 555 – 562

To link to this Article: DOI: 10.1080/02678299508036658

URL: <http://dx.doi.org/10.1080/02678299508036658>

PLEASE SCROLL DOWN FOR ARTICLE

Full terms and conditions of use: <http://www.informaworld.com/terms-and-conditions-of-access.pdf>

This article may be used for research, teaching and private study purposes. Any substantial or systematic reproduction, re-distribution, re-selling, loan or sub-licensing, systematic supply or distribution in any form to anyone is expressly forbidden.

The publisher does not give any warranty express or implied or make any representation that the contents will be complete or accurate or up to date. The accuracy of any instructions, formulae and drug doses should be independently verified with primary sources. The publisher shall not be liable for any loss, actions, claims, proceedings, demand or costs or damages whatsoever or howsoever caused arising directly or indirectly in connection with or arising out of the use of this material.

Stationary noise of the light scattered by a polymer-dispersed liquid crystal

by P. ALLIA*, C. OLDANO, M. RAJTERI, P. TAVERNA and L. TROSSI

Dipartimento di Fisica, Politecnico di Torino, 10129 Torino, Italy
Consorzio INFM, Research Unit of Torino Politecnico, 10129 Torino, Italy

and R. ALOE

Dipartimento di Chimica, Università della Calabria, 87036 Rende, Italy
Consorzio INFM, Research Unit of Cosenza, 87036 Rende, Italy

(Received 3 May 1994; accepted 7 June 1994)

Room temperature measurements of the stationary noise of the monochromatic light scattered by a polymer-dispersed liquid crystal (PDLC) have been performed in order to get information about the parameters affecting the fluctuation modes within the LC droplets, such as the effective viscosity constant of the anisotropic medium. The power spectra of the scattered light appear to be described in terms of lorentzian functions, whose intensity and cut-off frequency are strongly dependent on both the scattering angle and the electric field across the sample. Hints about the optical-axis configuration within the LC droplets are provided by a thorough analysis of the measured noise. The main discrepancies between the experimental results and the predictions for an infinite nematic LC are pointed out and discussed in terms of the finite size of the LC droplets.

1. Introduction

A considerable research effort has been recently addressed to the study of polymer-dispersed liquid crystals (PDLCs), mainly because of their present or prospective applications in electro-optical displays or in light shutters [1]. A PDLC is essentially an assembly of non-interacting droplets of a nematic liquid crystal embedded in a polymer matrix. For practical applications, the droplet size must be in the micrometer range [1]. Most of the research done in this area is concerned with relevant physical parameters for a PDLC to be used in applications, such as the switching voltage and the response time [2]. However, these composite optical media are worthy of attention also from a more fundamental viewpoint. Finite-size effects play in fact a central role in determining both the equilibrium configuration of the director within each droplet, and its response to an applied field (either electric or magnetic). Various models of the director's configuration in spherical or ellipsoidal droplets have been studied in detail [3-5]. However, many problems concerning the optical properties of a PDLC still remain open.

Measurement techniques based on the analysis of the light scattered by liquid crystals have proved to be a powerful tool to investigate the structure of this class of

anisotropic media [6]. Light scattering phenomena in PDLC have been examined with particular attention, owing to the role played by these effects in determining the contrast of electro-optical devices based on PDLC technology. The scattering profiles of droplets characterized by the most common configurations of the director have been thoroughly analysed [7, 8]. The role of multiple scattering has also been discussed in some detail [9, 10]. The angular dependence of the intensity of the light scattered by a typical PDLC has been calculated and experimentally checked [11].

However, the study of the properties of the light scattered by a nematic liquid crystal may also provide interesting information on more fundamental aspects of the considered medium. As is well known, the stationary noise of the light scattered at a given angle by a NLC arises from the thermal fluctuations of the director [6] and may be exploited to get information about the elastic and viscous constants of the material [12]. The same information can in principle be obtained in the case of a PDLC. However, to our knowledge no information about the existence and characteristics of the noise of the monochromatic light scattered by a PDLC is presently available.

The aim of this work is to study the stationary noise of the light scattered by a typical PDLC submitted to an electric field. This analysis allows one to discuss different

* Author for correspondence.

aspects of the considered material, such as the director's configurations within the droplets, the average droplet size, the average viscosity of the NLC, and the effect of the electric field on the dynamics of the fluctuation modes within droplets.

2. Experimental

Three samples of polymer-dispersed liquid crystals (PDLCs) were prepared using the polymerization-induced phase separation method. A homogeneous solution was obtained by adding the nematic liquid crystal (NLC) to a polymeric matrix. The solution was sandwiched between two glasses with spacers of $35\ \mu\text{m}$ and subsequently heated for a suitable time. Sample *A* was obtained by dispersing into a thermoplastic matrix the nematic liquid crystal (NLC) E7 (having dielectric and optical anisotropy $\varepsilon = 13.9$ and $\Delta n = 0.225$, respectively). In sample *B*, the NLC was RDE-01168 (Hoffmann-La Roche, Switzerland) with dielectric and optical anisotropy $\varepsilon_a = 7.39$ and $\Delta n = 0.159$, respectively; the polymeric matrix was Bostik. Finally, sample *C* was prepared using the same NLC as in sample *B*, while the polymer was a mixture formed by the Epoxide Resins Epon 828 (Miller-Stephenson, USA) and Heloxy WC 68 (Wilmington Chemical Corporation, USA) and the curing agent Capcure 3800 (Diamond Shamrock Corporation, USA). Sample *C* was heated at 80°C for 12 h.

All samples were submitted to an electric field and simultaneously observed through a polarizing microscope with cross polarizers, in order to get information on both the droplet sizes and the optical axis of different particles.

The experimental set-up for light-scattering measurements is shown in figure 1. The polarizer P_1 and the quarter-wave plate Q act as an optical isolator of the light emitted by the 10 mW He-Ne laser L . The laser beam is filtered and focused on the sample through the pinhole PH and the converging lens L_2 . The polarization of the light

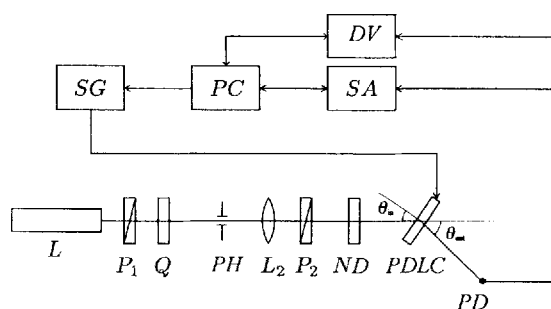


Figure 1. Experimental set-up for light scattering measurements. L : He-Ne laser; P_1 , P_2 : light polarizers; Q : quarter-wave plate; PH : pinhole; L_2 : converging lens; ND : neutral density filter; $PDLC$: sample; PD : photodiode; SA : spectrum analyser; DV : digital voltmeter; PC : computer; SG : signal generator.

is determined by the polarizer P_2 and the intensity is controlled through a suitable neutral density filter ND . The light emerging from the sample is detected by the photodiode PD , whose signal is amplified and sent either to the FFT signal analyser SA , providing the average power spectrum of the noise in the frequency range $2.5 \times 10^{-2} < \nu < 2 \times 10^4 \text{ Hz}$, or to the digital voltmeter DV , exploited in measurements of the intensity of diffracted light. These instruments and the signal generator SG , connected with the $PDLC$ cell, are controlled by the computer PC .

An electric field perpendicular to the plane of the samples was obtained by applying an oscillating voltage (frequency 10^3 Hz , intensity $0\text{--}10 \text{ V}$) to transparent ITO (indium-tin-oxide) electrodes deposited on the inner surface of the glasses. Higher voltages (up to 20 V) were obtained by means of a transformer. The photodiode was mounted on a platform rotating in the incident plane around a vertical axis coincident with the sample. The latter could independently rotate around the same axis in order to change the angle of incidence θ_i .

3. Results

3.1. Droplet size observation

The sizes and shapes of the droplets, observed through the polarizing microscope, were found to differ substantially from specimen to specimen. Sample *A* is composed of finely dispersed particles, whose average diameter (about $1\ \mu\text{m}$) could hardly be determined by direct observation. On the contrary, samples *B* and *C* contain much larger droplets, characterized by a broad size range (their transverse dimensions are distributed between 20 and $100\ \mu\text{m}$ in sample *B*, and between 10 and $40\ \mu\text{m}$ in sample *C*). In the latter specimen, most of the large droplets are definitely not spherical, with a rather large aspect ratio. Moreover, these large-size particles were often found to occupy the whole of the sample thickness, the separation between the inner glass surfaces being $35\ \mu\text{m}$, as discussed above. Note that the droplet size of specimens *B* and *C* would not match the requirements for the application of these samples as device components [1]. However, the emphasis of the present study is more on the general properties of these media than on their specific applications. From this viewpoint, the presence of large sized particles is not detrimental to the accuracy of the following analysis. Moreover, multiple scattering effects, predicted to play a dominant role in thick $PDLC$ samples composed of many particles [1], can be neglected in the present case.

3.2. Light-scattering measurements

The intensity of the scattering light, normalized to its maximum value, is reported in figure 2 as a function of the

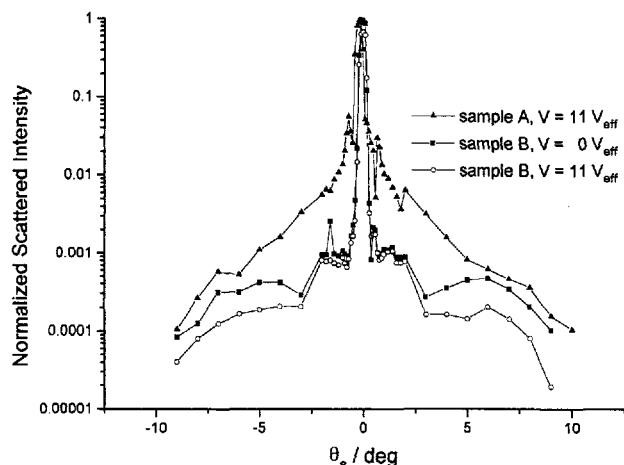


Figure 2. Normalized scattering intensity as a function of scattering angle θ_s in two polymer-dispersed samples for different values of the applied voltage (incidence angle $\theta_i = 50^\circ$).

scattering angle θ_s for two different polymer-dispersed liquid crystal systems (samples A and B). The effect of an applied external field is also shown. All curves were obtained under normal incidence of light. In each case, the intensity of the scattered light is observed to decrease rapidly with increasing θ_s , with a behaviour already observed or predicted in similar media [11]. Actually, the intensity of the scattered light appears to be more dependent on the size and composition of the drops than on the value of the applied field. Note the complex intensity oscillations observed in both samples—in turn narrow and sharp at low θ_s values, and broad and shallow at larger angles—related to light-diffraction effects.

3.2. Power spectra of the scattered light

Typical power spectra of the stationary noise of the light scattered from sample C for an incidence angle of 50° in air are shown in figure 3 (a) and (b) for selected values of the scattering angle and of the voltage applied to the sample, respectively. The incidence angle was chosen to avoid any contribution from the direct beam to the light picked by the photodiode. Generally speaking, the spectra appear to be characterized by a lorentzian shape, as expected in this case [12]. Each spectrum was therefore routinely fitted by a lorentzian function (dashed lines in figure 3), allowing one to determine the low frequency spectral density and the cut-off frequency Γ . A lorentzian shape was observed at low fields for the spectra detected in all the sample regions examined, although small differences in the fitting parameters were found by exploring different areas, indicating the existence of large scale inhomogeneities in the droplet sizes. Note that the spot diameter on the target was of the order 1 mm, i.e.

much larger than the maximum droplet size (about $40 \mu\text{m}$ in this sample).

The behaviour of the cut-off frequency of the power spectra is shown in figure 4 as a function of $\sin(\theta_s/2)$, for selected values of the applied voltage V_{eff} . All experimental curves are well described by a general power law of the type $\Gamma = a[\sin(\theta_s/2)]^b + c$, where all coefficients are found to be dependent on the applied voltage. The best-fit values of the parameters a , b and c corresponding to the dashed lines in figure 4, are reported in the table. In particular, the parameter c is observed to vary according to the square of V_{eff} , as observed in figure 5. In the absence of an applied field, the experimental Γ versus $\sin(\theta_s/2)$ curve ostensibly deviates from a pure power-law behaviour at low scattering angles, as shown in figure 6.

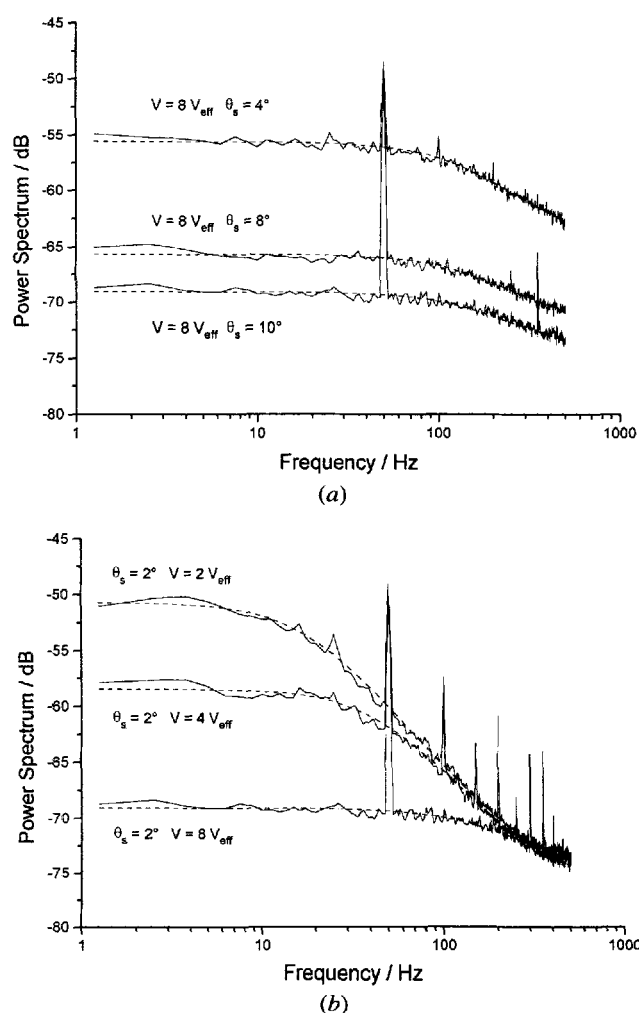


Figure 3. Representative power spectra of the light scattered from sample C: (a) for three different scattering angles at $V = 8 V_{\text{eff}}$ and $\theta_i = 50^\circ$, (b) for three different voltage values at $\theta_s = 2^\circ$ and $\theta_i = 50^\circ$. Dashed lines: lorentzian best-fit curves.

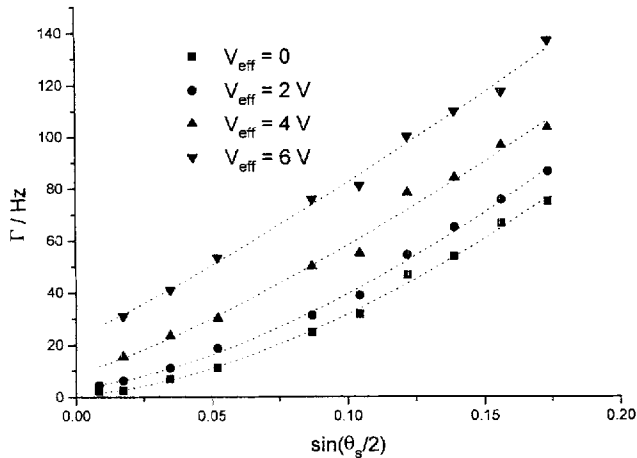


Figure 4. Cut-off frequency Γ of lorentzian power spectra of the scattered light versus $\sin(\theta_s/2)$ (proportional to the transferred wavevector) for different voltage values and $\theta_i = 50^\circ$. Dotted lines: best-fit curves (see text).

Parameters obtained by fitting the $\Gamma[\sin(\theta_s/2)]$ curves to a generalized power law, $\Gamma = a[\sin(\theta_s/2)]^b + c$, for different voltage values and $\theta_i = 50^\circ$.

V_{eff}/V	a/Hz	b	c/Hz
0	1305	1.629	0.970
2	1255	1.548	4.009
4	848	1.241	9.473
6	808	1.140	23.825

The effect of an electric field on the lorentzian power spectra of the light scattered by sample *C* is shown in figures 7 to 9. The behaviour of the cut-off frequency Γ is reported in figure 7 as a function of the applied voltage V for $\theta_i = 50^\circ$ and for three representative scattering angles. The experimental data are well fitted by a law of the type $\Gamma = \alpha V^2 + \beta$, at least for low voltages (dashed lines in figure 7). A similar behaviour can actually be found for all examined scattering angles. The coefficient α of the parabolic law turns out to be an increasing function of θ_s , as observed in figure 7 and more clearly shown in figure 8, where α is plotted against $\sin(\theta_s/2)$. The parameter α displays a tendency towards saturation for large values of $\sin(\theta_s/2)$.

The effect of the field on the amplitude of the fluctuation modes of the director may be clearly observed in figure 9, where the relative change in the low-frequency spectral density is plotted as a function of V for selected values of θ_s and $\theta_i = 50^\circ$. Note that the reported amplitudes have been obtained by subtracting, for each scattering angle, the corresponding zero-field value, which is strongly dependent on θ_s . Generally speaking, an electric field acts to reduce the low-frequency fluctuations of the director, the

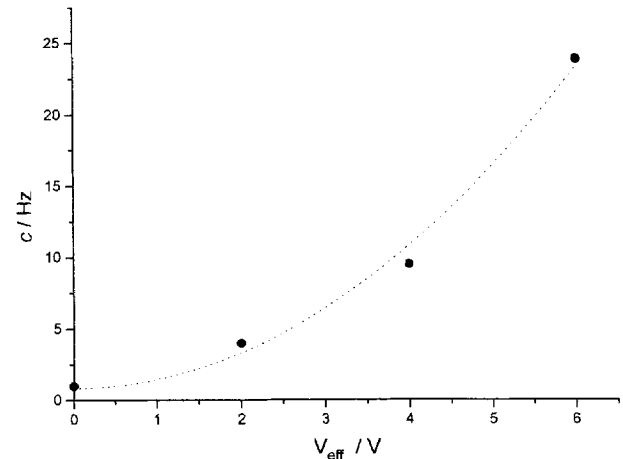


Figure 5. Fitting parameter c of the $\Gamma[\sin(\theta_s/2)]$ curves versus applied voltage. Dashed line: quadratic best-fit curve.

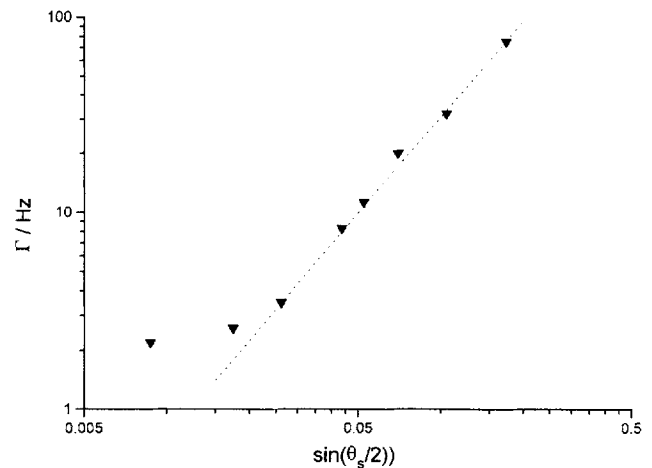


Figure 6. Logarithmic plot of the cut-off frequency Γ versus $\sin(\theta_s/2)$ ($V_{\text{eff}} = 0$). Dashed line: parabolic best-fit curve.

effect becoming increasingly relevant with reducing scattering angle.

Finally, the effect of a large electric field on the spontaneous fluctuations of the director is shown in figure 10, where the cut-off frequency of the spectra measured on sample *C* is reported as function of V for $\theta_i = 50^\circ$ and for two representative scattering angles. In both cases, a parabolic increase of Γ with V_{eff} is observed for low voltage values ($V_{\text{eff}} < 8$ V). Minor differences with respect to the corresponding curves of figure 3 are related to the choice of another region of the sample. For high voltage values, however, the experimental curves largely deviate from the parabolic behaviour, and the cut-off frequency is observed to decrease with increasing V_{eff} . The effect is most evident at low scattering angles, where the high-field values of Γ become comparable to the value found when $V_{\text{eff}} = 0$. As a matter of fact, for $V_{\text{eff}} > 10$ V,

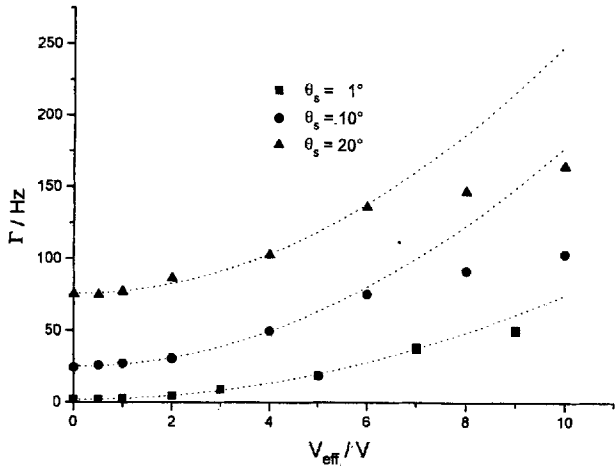


Figure 7. Cut-off frequency Γ versus applied voltage for three different scattering angles and $\theta_i = 50^\circ$. Dotted lines: parabolic best-fit curves based upon low voltage data.

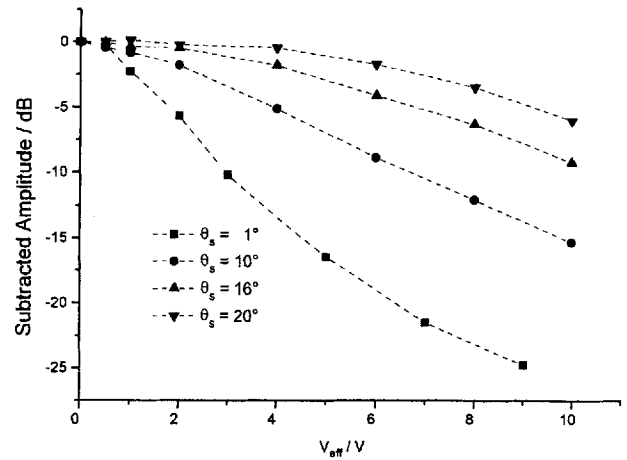


Figure 9. Subtracted low-frequency spectral densities versus applied voltage for different values of the scattering angle and $\theta_i = 50^\circ$.

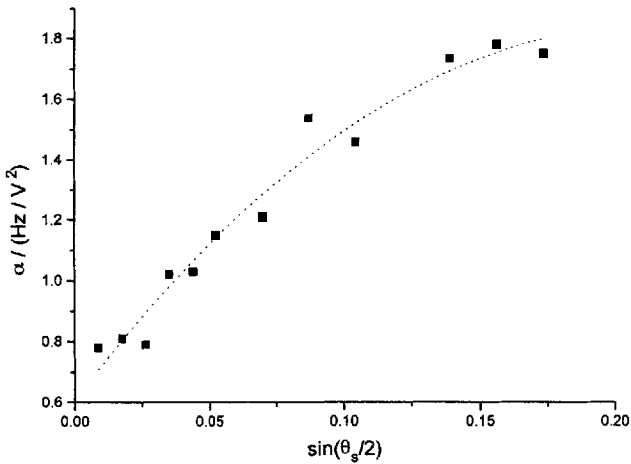


Figure 8. Fitting parameter α of the $\Gamma(V_{\text{eff}})$ curves versus $\sin(\theta_s/2)$. The dashed line is a guide for the eye.

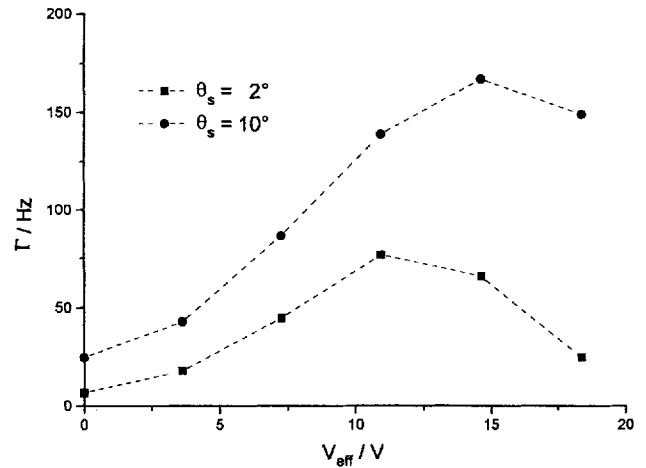


Figure 10. High-voltage behaviour of the cut-off frequency Γ for two representative scattering angles and $\theta_i = 50^\circ$.

the measured spectra begin to deviate considerably from the Lorentzian shape typical of these measurements, and display an increasing tendency towards a less steep frequency behaviour, essentially a $1/f$ decay. As a consequence, the values of Γ reported for high V_{eff} values in figure 10, and still obtained by a fit to a Lorentzian function, should be regarded as merely suggestive of a significant change in the mode dynamics.

4. Discussion

The differences observed in the time-averaged intensity of the scattered light, plotted against θ_s in figure 2, clearly reflect both the intrinsic features of the droplet constituents and the different sizes of the particles dispersed in the samples. The latter effect seems to be dominant. In fact, sample A, characterized by a drop diameter of the

order $1 \mu\text{m}$, gives rise to a much broader curve than sample B, as expected on the basis of simple considerations. However, the time-averaged intensity of the scattered light seems not to be particularly sensitive to external parameters, as noticed by considering the rather weak effect of an electric field on the scattered intensity (see figure 2). Apparently, much higher fields should be applied to obtain relevant changes in the measured curves. More significant information on the peculiar features of PDLCs can however be obtained by studying the stationary fluctuations of the director through the spectral analysis of the noise of the light scattered by the sample.

As is well known, in thin liquid crystal samples the mean amplitude of the thermal fluctuations of the director is related to the intensity of the restoring forces, and is directly proportional to the mode wavelength $\lambda_m = 2\pi/q$,

q being the modulus of the wavevector transferred in a typical scattering measurement. The restoring forces acting on an ideal sample (where all boundary effects are neglected) are mainly elastic forces, parameterized by the three Frank constants, and electric forces, related to the anisotropy of the dielectric constant ϵ_a . Under these conditions, the power spectrum of the light scattered by an infinite liquid crystal sample is predicted to be characterized by a Lorentzian shape with a cut-off frequency

$$\Gamma = \frac{\bar{K}q^2 \pm \frac{1}{2}\epsilon_a E^2}{\bar{\eta}} \quad (1)$$

where \bar{K} is a proper linear combination of three Frank constants and $\bar{\eta}$ is a generalized viscosity coefficient. The transferred wavevector q is related to the scattering angle θ_s through the relation $q = 2\bar{n}k \sin(\theta_s/2)$, where $k = 2\pi/\lambda$, λ being the wavelength of the incident light, and \bar{n} is the average refractive index of the medium. The plus sign in equation (1) is used when the unperturbed director is parallel to the electric field (as in homeotropic NLC), while the minus sign applies in the case of a planar NLC.

The validity of equation (1) has been checked on various nematic liquid crystals [13–15]. As a consequence, the spectral analysis of the scattered light intensity fluctuations has become a standard technique to measure the ratio of the elastic to viscous constants, the ratio of the Frank constants to the anisotropy of the dielectric constant, and, under particular conditions, the absolute value of the viscous and friction constants [12]. In all mentioned cases, however, all effects related to the finite size of the samples were negligible. The present measurements were instead performed on systems where the surface-to-volume ratio of the liquid crystal may be much higher than in other cases. Surface effects are therefore inherent to the considered medium. Moreover, the droplet size in the considered PDLCs appears to be distributed over a broad range. As a consequence, varying the angle of observation of the scattered light allows one to discriminate, to a certain extent, the contributions from the various droplets according to their size. In fact, measurements at very low θ_s ($\theta_s \approx 1^\circ$) give information on the long wavelength fluctuation modes within the droplets having the largest sizes. On the contrary, the noise detected at high scattering angles contains entangled contributions from both the large droplets (short wavelength modes) and from the small ones.

In the light of the peculiar features of the examined medium and of the measured noise, one could expect that equation (1) may lose validity. In fact, the results reported in figure 4 clearly show that the dependence of Γ on q^2 predicted by equation (1) no longer holds, although the data still appear to be fitted by a power law of the type $\Gamma = a'q^b + c$. It should be noted that the coefficient b steadily increases with decreasing θ_s up to a value of about

1.63 for $\theta_s = 1^\circ$, corresponding to the contribution from the largest droplets (see the table). On the other hand, figure 5 shows that even in this case, the coefficient c is proportional to the square of the applied field, as predicted by equation (1).

The finite dimensions of the scatterers are responsible for the deviation from a pure power law observed when $V = 0$. In this case, the parameter c should vanish. However, no modes with wavelength longer than the maximum droplet size can exist, so that there must be a minimum value in the transferred wavevector, and therefore in Γ . An estimate of the maximum droplet size, d_{\max} , may be made by using the approximate relation $q_{\min} \approx \sqrt{(3)\pi}/d_{\max}$. As a consequence, $d_{\max} \approx \sqrt{(3)\pi}/(\Gamma_{\min}/a')^{1/b}$, where $a' = a/(2k\bar{n})^b$. By using $\lambda = 0.6328 \mu\text{m}$, $\bar{n} = 1.5$, $a = 1.3 \times 10^3 \text{ Hz}$, $b = 1.63$, $\Gamma_{\min} = 1 \text{ Hz}$, one gets $d_{\min} \approx 15 \mu\text{m}$. This is the average droplet size in the examined region, in good agreement with direct observations.

The adequacy of equation (1) to explain the dependence of Γ on the applied field, suggested by the behaviour of the parameter c in figure 5, is confirmed by the results reported in figure 7, at least for low voltage values, where it is always possible to fit the Γ versus V_{eff} curve to a parabola with upward concavity. This means that in these measurements, the NLC director is predominantly perpendicular to the sample plane, irrespective of the droplet size. In fact, direct observation shows that in large droplets, the NLC is predominantly perpendicular to the plane of the sample even at $V = 0$, possibly owing to interactions with the glass substrates. Deviations from this alignment are observed to occur only in relation to the rest of the surfaces of these very large particles. Smaller droplets can in principle be characterized by a radial or a bipolar configuration of the director [1] when $V_{\text{eff}} = 0$. In the latter case, an essentially random distribution of the optical axes of the droplets is expected. If the optical axes were not modified by the applied field, the observed behaviour of Γ with V_{eff} should differ from a simple parabolic law with upward concavity when contributions from smaller droplets are included in the measured spectra (i.e. at large scattering angles). The present results indicate instead that the optical axes of all droplets are essentially aligned along the electric field over the whole voltage range explored. As a consequence, the switching voltage V_B for these particles must be very low. This result points to a bipolar configuration of the director in the PDLC studied [1]. As a matter of fact, the switching voltage in a bipolar droplet may be calculated according to the formula

$$V_B = \frac{d}{3a} \left(\frac{\epsilon_{lc}}{\epsilon_p} + 2 \right) \left(\frac{K(l^2 - 1)}{\epsilon_a} \right)^{1/2}, \quad (2)$$

where d is the sample width, a is the average droplet radius ϵ_{lc}/ϵ_p is the ratio between the liquid crystal and the polymer

low frequency dielectric constants, K is an effective elastic constant, l is the ratio between the major and minor axes of a slightly prolate droplet and ϵ_a is the anisotropy of dielectric constant [2]. By taking $(\epsilon_{ic}/\epsilon_p) \approx 5$, $K \approx 5 \times 10^{-12} \text{ N}$, $l \approx 1.1$, and $\epsilon_a \approx 7.4 \epsilon_o \approx 6 \times 10^{-11} \text{ C}^2 \text{ Nm}^{-2}$, one gets $V_B \approx 2 \text{ V}$ for droplets with $a \approx 5 \mu\text{m}$, even lower V_B values being predicted for larger particles. The observed behaviour of Γ with V_{eff} is therefore compatible with the hypothesis that the PDLC is composed of droplets with a bipolar configuration of the director, essentially aligned along the electric field. It should be noted, however, that light scattering measurements show that the droplet directors are not perfectly aligned even by a voltage significantly higher than V_B , possibly owing to shape effects [16].

In an infinite sample the coefficient α of the parabolic $\Gamma(V_{\text{eff}})$ curve is independent of θ_s , and allows one to obtain information on the effective viscosity constant $\bar{\eta}$ if the value of ϵ_a is measured independently. An order of magnitude estimate of $\bar{\eta}$ may be obtained even in the present case, although α is now a function of θ_s , provided that the optical signal arises from the large droplets, where surface energy effects may be assumed as almost negligible to a first approximation. Spectral analysis at low scattering angles provides such information. At the large droplets, the sample behaves as a plane capacitor with a dielectric substance kept at constant applied voltage. The electric field within the liquid crystal is then simply given $E = V/d$, $d = 35 \mu\text{m}$ being the sample thickness. One therefore gets

$$\bar{\eta} = \frac{1}{2\alpha} \frac{\epsilon_a}{d^2} \approx 3.31 \times 10^{-2} \text{ kg m}^{-1} \text{ s}^{-1} \quad (3)$$

using $\alpha = 0.74 \text{ Hz V}^{-2}$ when $\theta_s = 1^\circ$. This value of $\bar{\eta}$ (corresponding to 0.331 Poise) obtained is in good agreement with effective viscosity constants measured on similar nematic liquid crystals (MBBA) [6]. The agreement confirms that large droplets may be assumed to behave like a nearly infinite medium.

The experimental dependence of α on θ_s (see figure 8) may indicate that the overall alignment of the optical axis along the electric field is slightly higher when the contributions from smaller particles are taken into account (as in measurements at large θ_s) than when the diffracted light arises only from the long wavelength fluctuation modes of very large droplets.

It is interesting to note that for $V_{\text{eff}} > 10 \text{ V}$, the cut-off frequency definitely deviates from the parabolic behaviour, the relative reduction in Γ being stronger at low scattering angles. Although the low frequency spectral density is severely reduced in these conditions (see figure 9), there is sufficient experimental evidence to allow one to draw significant conclusions. As already noted, at high applied voltages, the spectra of the scattered light noise

lose their lorentzian character, gradually transforming into $1/f$ spectra. However, fitting these curves with lorentzians appears still to be possible to a first approximation, and leads to the data reported in figure 10. The results point to a field-induced softening of the fluctuation modes within the droplets. The appearance of $1/f$ spectra reflects a significant change in the degree of correlation among fluctuating modes, indicating that at high fields, the usual picture of nearly independent fluctuation events must be discarded. This behaviour may reflect the increasing role played by the droplet surface energy when the applied field becomes so high that the droplet shape and that static configuration of the director begin to be distorted. In such conditions, a fluctuation of the director at one point may rapidly induce similar fluctuations at neighbouring points, in order more efficiently to reduce the associated increase in free energy. Consequently, the degree of space- and time-correlations among single fluctuations increases, and their relaxation times become longer. A quantitative analysis of this effect however requires more experimental data than are presently available.

5. Concluding remarks

The measurements described in this paper show that an analysis of the thermal noise of the light scattered by a PDLC is a suitable tool to study various features of this novel class of media. In fact, the measured spectra give information not only on the average droplet size, but also on the dynamics of the modes of the dispersed LC. Generally speaking, the distinctive features of these spectra are not different in the PDLC specimen considered (sample C) from those for conventional slab-type samples of nematics. In particular, the spectral density usually appears to be a Lorentzian function of the measurement frequency, with a well defined cut-off frequency Γ . It should however be noted that the results of this spectral analysis only concern the optical axis fluctuations in large droplet PDLC films like those considered here.

An advantage of the present technique over conventional scattering measurements is that the scattered light noise appears to be much more sensitive to small changes of an external parameter (in this case an electric field) than the intensity of the scattered light. As a consequence, it has been possible to exploit the dependence of Γ on the applied voltage, in order to get significant information about the effective viscosity parameter of the NLC contained in the largest droplets. The role of the finite droplet size and related surface effects has been evidenced by comparing some aspects of the experimental curves with the predictions for an infinite NLC. In particular, the degree of correlations among fluctuating modes has been found to increase strongly at high voltage values.

Finally the proposed technique allows one to get information on the nature of the director configuration

within the droplets. In the present case, the experimental dependence of Γ on V_{eff} indicates a very low switching voltage V_B for the LC molecules in all droplets, a feature suggesting that the starting configuration of the director is of a bipolar type in this PDLC.

References

- [1] DOANE, J. W., 1991, *Liquid Crystals—Applications and Uses*, Vol. 1, edited by B. Bahadur (World Scientific), p. 361.
- [2] ERDMANN, J., DOANE, J. W., ZUMER, S., and CHIDICHIMO, G., 1989, *Proc. SPIE*, **1080**, 32.
- [3] VOLOVIK, G. E., and LAVRENTOVICH, O. D., 1983, *Soviet Phys. JETP*, **58**, 1159.
- [4] GOLEMME, A., ZUMER, S., DOANE, J. W., and NEUBERT, M. E., 1988, *Phys. Rev. A*, **37**, 559.
- [5] DRZAIĆ, P. S., 1988, *Liq. Crystals*, **3**, 1543.
- [6] DE GENNES, P., 1975, *The Physics of Liquid Crystals* (Clarendon Press), p. 59.
- [7] ZUMER, S., and DOANE, J. W., 1986, *Phys. Rev. A*, **34**, 3373.
- [8] ZUMER, S., 1988, *Phys. Rgv. A*, **37**, 4006.
- [9] ZUMER, S., GOLEMME, A., and DOANE, J. W., 1989, *J. opt. Soc. Am. A*, **6**, 403.
- [10] MONTGOMERY, G. P., 1988, *J. opt. Soc. Am. B*, **5**, 774.
- [11] VAZ, N. A., SMITH, G. W., and MONTGOMERY, G. P., 1987, *Molec. Crystals liq. Crystals*, **146**, 1.
- [12] MIRALDI, E., TROSSI, L., TAVERNA VALABREGA, P., and OLDANO, C., 1980, *Nuovo Cim. B*, **60**, 165.
- [13] ORSAY LIQUID CRYSTAL GROUP, 1969, *Phys. Rev. Lett.*, **25**, 1361.
- [14] FELLNER, H., FRANKLIN, W., and CHRISTENSEN, S., 1975, *Phys. Rev. A*, **11**, 1440.
- [15] VAN ECK, D. C., and WESTERA, W., 1977, *Molec. Crystals liq. Crystals*, **38**, 319.
- [16] WHITEHEAD, J. B., ZUMER, S., and DOANE, J. W., 1989, *Proc. SPIE*, **1080**, 3.